

Structures, Dynamic Behavior, and Spectroscopic Properties of 1,8-Anthrylene–Ethenylene Cyclic Dimers and Their Substituent Effects¹

Masataka Inoue,¹ Tetsuo Iwanaga,¹ and Shinji Toyota*²

¹Department of Chemistry, Faculty of Science, Okayama University of Science, 1-1 Ridaicho, Kita-ku, Okayama 700-0005

²Department of Chemistry and Materials Science, Tokyo Institute of Technology, 2-12-1 Ookayama, Meguro-ku, Tokyo 152-8551

E-mail: stoyota@cms.titech.ac.jp

Received: July 17, 2015; Accepted: August 14, 2015; Web Released: August 21, 2015



Shinji Toyota

Professor Shinji Toyota studied chemistry at The University of Tokyo and received Master's degree in 1988. He became research assistant of Okayama University of Science in 1988. After he received Doctor's degree in 1992 from The University of Tokyo, he was promoted to professor in 2002. He stayed in University of California, San Diego as visiting researcher in 1996–1997. In 2015, he moved to Tokyo Institute of Technology as professor. He is interested in physical organic chemistry, structural organic chemistry, and stereochemistry.

Abstract

Cyclic compounds consisting of two 1,8-anthrylene units and two ethynylene linkers were studied as π -conjugated compounds. Three derivatives having substituents (H, Me, and Ph) at the linker moieties were synthesized by Suzuki–Miyaura coupling of the corresponding diethynylanthracene boronic esters with 1,8-diiodo-10-mesitylanthracene. The X-ray analysis and DFT calculations revealed that all the compounds had nonplanar cyclic frameworks where the two ethynylene linkers were *syn* to the anthracene units. Exchanges between the two *syn* forms were observed from the line shape changes in the ¹H NMR signals of the mesityl group. Their barriers increased in the order of H, Ph, and Me compounds from 34 to 70 kJ mol⁻¹. The effects of substituents on the molecular structure, dynamic behavior, and electronic properties are discussed.

We have concentrated our efforts on studies of cyclic oligomers consisting of anthracene units and acetylene linkers as novel π -conjugated compounds for about ten years.² Based on the molecular designs, we have constructed a large number of fascinating cyclic systems by modifying the number of aromatic units and the position and length of acetylene linkers. We have synthesized cyclic oligomers ranging from dimers to dodecamers having U-turn shaped 1,8-anthrylene units.² As the smallest cyclic oligomer, we reported cyclic dimer **1** (Figure 1) with two ethynylene linkers (–C≡C–), which featured a rigid and planar framework that produced characteristic absorption and emission spectra.^{3,4} In the molecular design of π -conjugated

systems, *trans*-ethynylene linkers (–CH=CH–) have also been occasionally utilized to connect the aromatic moieties.⁵ Because this double bond linker has a nonlinear zigzag shape, the chain shape and the conjugation are dependent on the conformation about the single bonds. For anthrylene–ethynylene oligomers, some acyclic and cyclic analogs were reported as novel fluorophores and twisted systems.⁶ Another example of a cyclic compound is **2**, which was synthesized as a fused [14]annulene in 1971 by Akiyama and Nakagawa.⁷ Although the authors proposed a nonplanar structure on the basis of electronic spectra, this cyclic compound has not been further investigated for more than 40 years.

In order to revisit this compound, we introduced a 2,4,6-trimethylphenyl (mesityl or Mes) group at the 10-position of one of the anthracene units. This bulky group is known to improve the solubility and stability of the attaching aromatic moieties because it offers steric protection from molecular stacking and external reagents.⁸ Another important role is that the two methyl groups at the 2,6-positions (*o*-Me) serve as a probe for the observation of dynamic behavior by NMR spectroscopy because the mesityl group is conformationally locked relative to the anthracene group.⁹ Therefore, we selected compound **3a** bearing an extra 10-mesityl group as the main target in the present study. We also synthesized its derivatives, **3b** and **3c**, which have methyl and phenyl groups at the linker moieties, respectively, and should influence the structures and properties of the macrocyclic compounds. We herein report the synthesis of soluble cyclic dimers **3** by cross coupling reactions and the substituent effects on their structures, dynamic behavior, and spectroscopic properties.

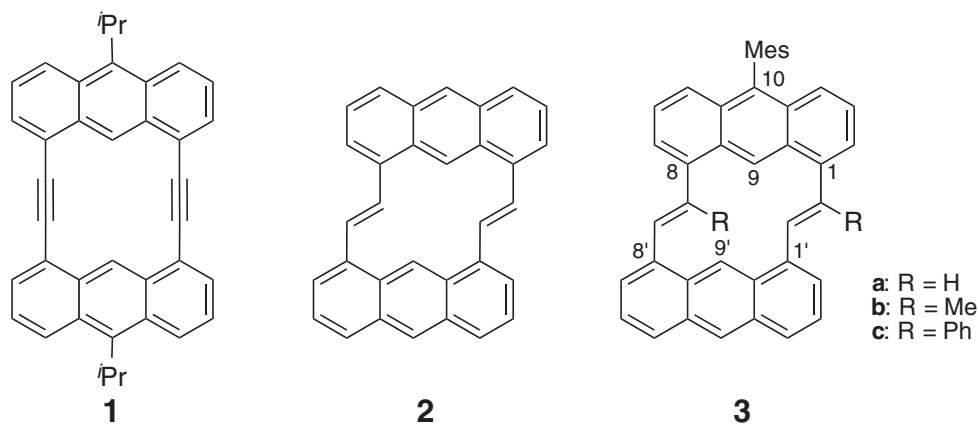
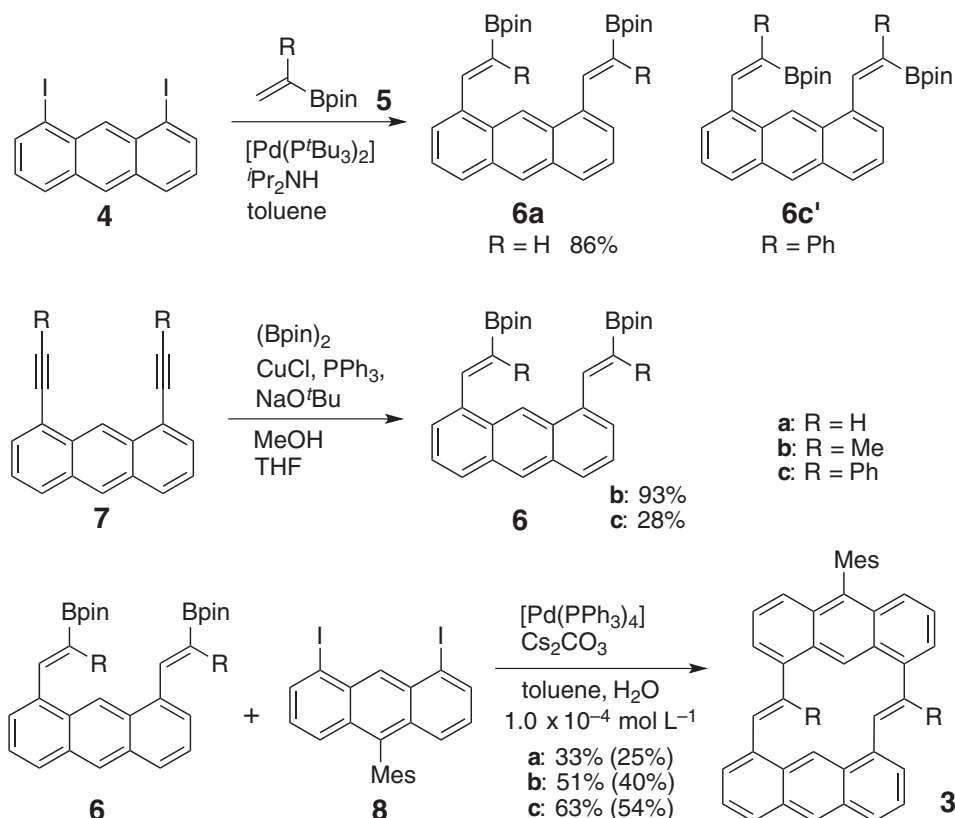


Figure 1. 1,8-Anthrylene cyclic dimers with various linkers (Mes: mesityl).



Scheme 1. Synthesis of cyclic dimers **3** (Bpin: 4,4,5,5-tetramethyl-1,3,2-dioxaborolan-1-yl group. Yields at $1.0 \times 10^{-3} \text{ mol L}^{-1}$ are given in parentheses).

Results and Discussion

Synthesis. Compound **2** had been synthesized by the Wittig reaction of dialdehyde and diylide of anthracene derivatives via several steps in the original literature.⁷ In order to decrease the number of reaction steps and facilitate the structural modification, we adopted cross coupling reactions. Compounds **3** were synthesized by cyclization via the Suzuki–Miyaura coupling of diboronic esters **6** and diiodoanthracene **8**¹⁰ (Scheme 1). Compound **6a** was readily prepared by the Heck reaction of 1,8-diiodoanthracene (**4**) and ethenylboronic ester **5a** in 86% yield.¹¹ This coupling reaction was also carried out with sub-

stituted boronic esters, but the reaction with **5b** proceeded very slowly and the reaction with **5c** gave undesired stereoisomer **6c'**.¹² Therefore, we utilized the addition reactions of 1,8-diethynylanthracene derivatives **7**. Although hydroborations of **7b** and **7c** with pinacolborane under some conditions were unsuccessful,¹³ the reactions with bis(pinacolate)diboron in the presence of CuCl gave the desired products in good yield for **6b** and in low yield for **6c**.¹⁴ In the latter case, the formation of regioisomers lowered the isolated yield of **6c**.

Thus prepared diboronic esters **6** were cyclized with **8**, which was prepared from 4,5-diiodo-9-anthrone and mesitylmagnesium bromide, by the Suzuki–Miyaura coupling. The

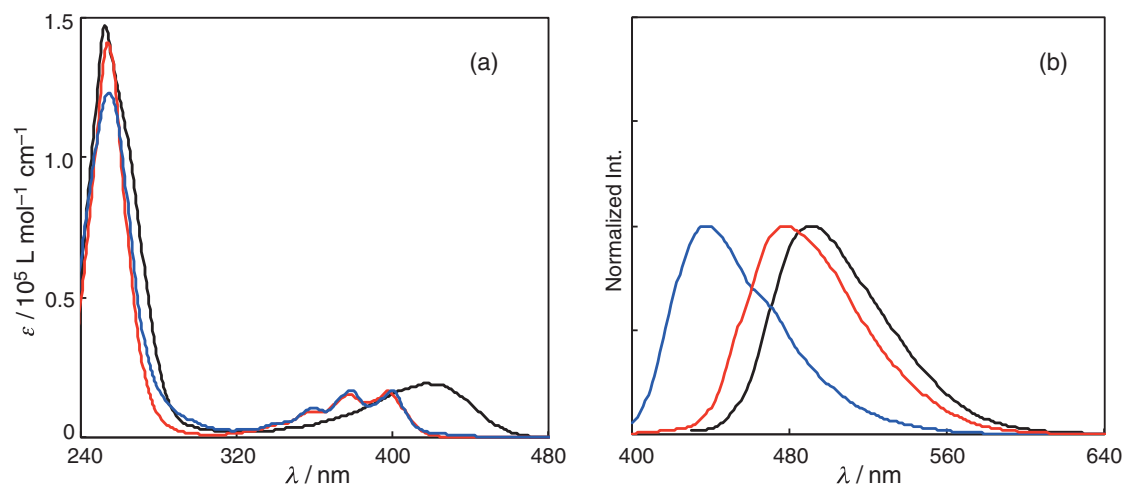


Figure 2. UV-vis (a) and fluorescence (b) spectra of **3a** (black), **3b** (blue), and **3c** (red) in CHCl_3 at $1.0 \times 10^{-5} \text{ mol L}^{-1}$ (UV-vis) and $1.0 \times 10^{-6} \text{ mol L}^{-1}$ (FL).

Table 1. UV-vis and fluorescence spectral data of **3** and **2** in chloroform

Compound	UV-vis		FL		Stokes shift /nm [cm^{-1}]
	$\lambda_{\text{max}}/\text{nm}$ (ϵ) ^a	$\lambda_{\text{edge}}/\text{nm}$ ^b	$\lambda_{\text{max}}/\text{nm}$	Φ_f ^c	
3a	417 (19000)	466	491	0.71	74 [3610]
3b	398 (16500)	421	438	0.82	40 [2300]
3c	400 (17000)	435	478	0.39	78 [4080]
2	413 (14800)	461	484	0.67	71 [3550]

a) Wavelengths and molar extinction coefficients of the absorption at the longest wavelength. b) Wavelengths at peak edge (5% intensity of the maximum peak). c) Absolute fluorescence quantum yield.

reaction with $[\text{Pd}(\text{PPh}_3)_4]$ as catalyst and Cs_2CO_3 as base afforded the desired cyclic products in moderate yields.¹¹ The yields were slightly increased to 33–63% under the low concentration conditions ($1.0 \times 10^{-4} \text{ mol L}^{-1}$). Compounds **3** were obtained as a yellow solid, and their structures were elucidated on the basis of spectroscopic data. Compound **2** was similarly synthesized from **6a** and 1,8-diiodoanthracene as reference compound. The molecular ion peaks were observed at the expected molecular weights, m/z 522.23 (**3a**), 550.27 (**3b**), and 674.30 (**3c**). In the $^1\text{H NMR}$ spectrum of **3a**, the signal due to alkene protons was observed as a singlet at δ 7.81, thereby offering no information on the coupling due to the coincidence of the chemical shifts of the two kinds of protons.¹⁵ Signals assignable to the inner protons at the 9-positions in **3a–3c** were observed in the low-field region (δ 9.6–10.1) due to the anisotropic effects of the double bond moieties at the 1,8-positions. The signal due to the *o*-Me groups in the mesityl group was observed as a singlet at δ 1.8 in all the compounds in CDCl_3 . In toluene- d_8 , the *o*-Me signals of **3b** and **3c** were observed as two broad singlets and a broad singlet, respectively. The broad signals suggest that the molecules undergo dynamic processes on the NMR time scale. These observations are analyzed and discussed later.

Electronic Spectra. The UV-vis absorption spectra and the fluorescence spectra of **3** were measured in chloroform (Figure 2 and Table 1). Compound **3a** showed a broad absorption band peaking at 417 nm and extending to 470 nm in the p-band region. This wavelength is comparable to that of parent compound **2**, indicating a very small effect of the 10-mesityl

substituent on the absorption spectra. Compounds **3b** and **3c** showed structured bands in this region, and the bands at the longest wavelength were blue-shifted by ca. 20 nm (peak) or ca. 40 nm (peak edge) relative to the peak of **3a**. This difference will be discussed later in terms of the molecular structure.

In the fluorescence spectra, compounds **3a** and **3c** as well as **2**¹ showed broad emission bands at 480–490 nm, resulting in large Stokes shifts at ca. 70 nm (ca. 3600 cm^{-1}). In contrast, a blue shift was notable for the emission of **3b**, and the Stokes shift was decreased to 40 nm (2300 cm^{-1}). These results mean that structural changes from the ground state to the excited state should be very large for **3a** and **3c**. Compounds **3** are highly emissive in solution; the absolute fluorescence quantum yields (Φ_f) of **3a** and **3b** are comparable to those of typical fluorescent anthracene compounds, such as 9,10-diphenylanthracene (0.90) and 9,10-bis(phenylethynyl)anthracene (0.87).¹⁶

Molecular Structures. The molecular structures of **3a–3c** and **2** were investigated by X-ray analysis and DFT calculations. Their ORTEP drawings are shown in Figure 3. All compounds have stair-like nonplanar macrocyclic frameworks, where two ethenylene moieties are directed to the same side of each anthracene plane (*syn* form). The conformation is characterized by the dihedral angles between the ethenylene moieties and the anthracene planes. The averages of the four angles (absolute values) at the acute angle corners are rather small (40 – 47°) for **3a** and **2** and large (73 – 79°) for **3b** and **3c**. Therefore, the substituents at the linker positions increased the dihedral angles via the steric hindrance, and it led to the decreased π -conjugation in the cyclic system. This structural

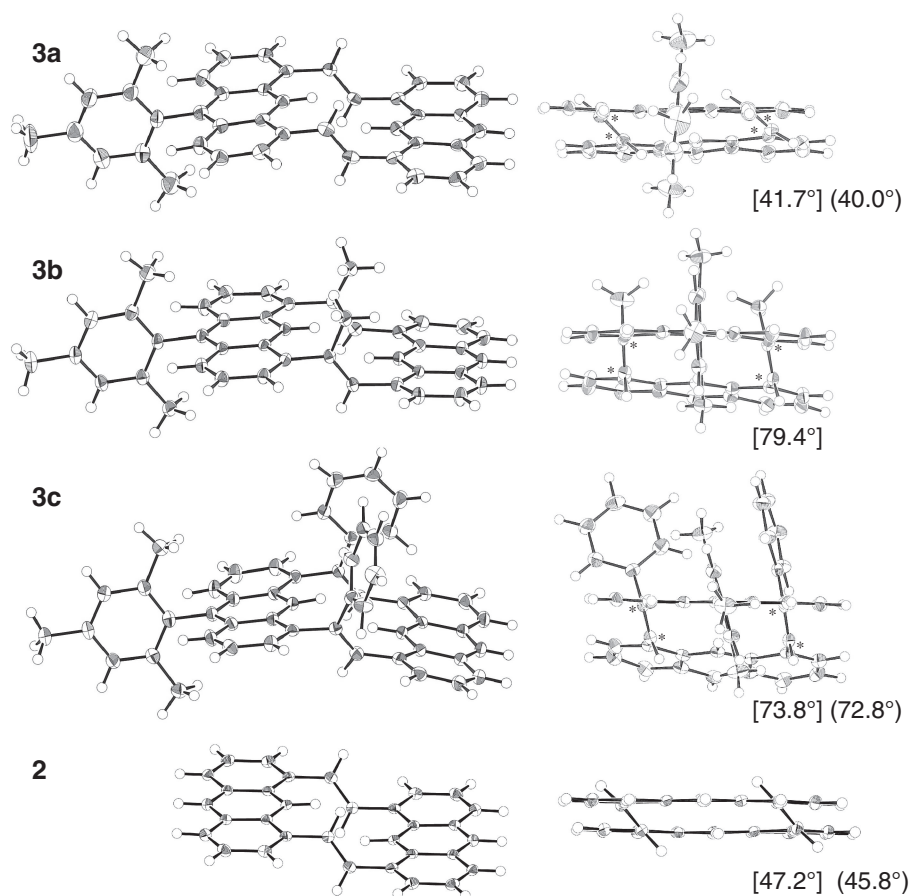


Figure 3. Two views of ORTEP drawings of compounds **3a–3c** and **2** (Solvent molecules are omitted. One of the two independent molecules for **3a**, **3c**, and **2**. Values in brackets are the averaged angles of the four dihedral angles marked by an asterisk (*), and those in parentheses are values for another independent molecule).

feature is consistent with the blue shift in the absorption spectra of **3b** and **3c**. The mesityl group in **3** is nearly perpendicular to the attaching anthracene plane (dihedral angle 75–88°). In **3c**, one phenyl group is nearly coplanar to the ethynylene group, whereas the other phenyl group is twisted by ca. 80° to form an intramolecular C–H... π contact at ca. 3.0 Å between the two phenyl groups.¹⁷

Figure 4 shows the packing diagrams of the X-ray structures of **3a** and **2**. For **3a**, no significant intermolecular π ... π contacts are observable, and the molecules loosely interact with one another via mainly C–H... π contacts. The mesityl groups form a column in the crystal lattice, where the solvent (benzene) molecules are included in the cavities. The packing modes of **3b** and **3c** are similar to that of **3a**. Compound **2** shows a typical herringbone packing, where the molecules form a linear network via π ... π interactions. The distance between the interacting anthracene planes is ca. 3.4 Å, which is comparable to the sum of the van der Waals radii of aromatic carbons. The difference in the crystal packing unambiguously indicates that the mesityl groups in **3a** prevent the molecules from forming tight intermolecular interactions in the crystal, thus increasing the solubility.⁸

DFT calculations of **3** were carried out at the M05/6-31G* level of theory.¹⁸ We obtained two energy-minimum structures, *syn* and *anti* forms, that differed in the conformation

of the linker moieties for each compound (Figure 5). The two ethynylene moieties are nearly parallel in the *syn* forms, whereas they are crossed in the *anti* forms. The X-ray structures are mostly reproduced by the calculation in the *syn* forms even though there is a difference in the conformation of the phenyl groups in *syn-3c*, which would be readily influenced by the packing effect in the X-ray structure. In all the compounds, the *syn* forms were more stable than the *anti* forms, where the energy differences ΔE were 9.0–11.1 kJ mol⁻¹ (Table 2). These values mean that compounds **3** mostly exist in the *syn* form under ordinary conditions.

MO Analysis. To obtain further insight into the effects of the molecular structures on the π -conjugation, we analyzed the molecular orbitals calculated at the same level. The HOMO and LUMO plots of **3** are shown in Figure 6. The orbitals are spread over the macrocyclic framework at the HOMO and LUMO levels for **3a**. Therefore, the conjugation of the anthracene units is extended across the ethynylene linkers leading to bathochromic effects on the p-band absorption due to the HOMO→LUMO excitation. In contrast, the orbitals are mainly located on one or two anthracene unit(s) and not extended across the ethynylene moieties at the HOMO and LUMO levels for **3b** and **3c**. This orbital distribution indicates that the π -conjugation is disconnected at the ethynylene linkers in the nearly bisected conformation. We also calculated the absorp-

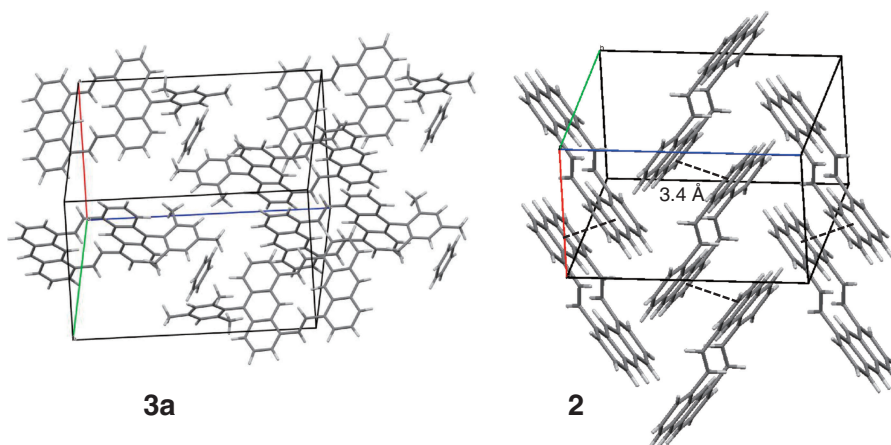


Figure 4. Packing diagrams of X-ray structures of **3a** and **2**.

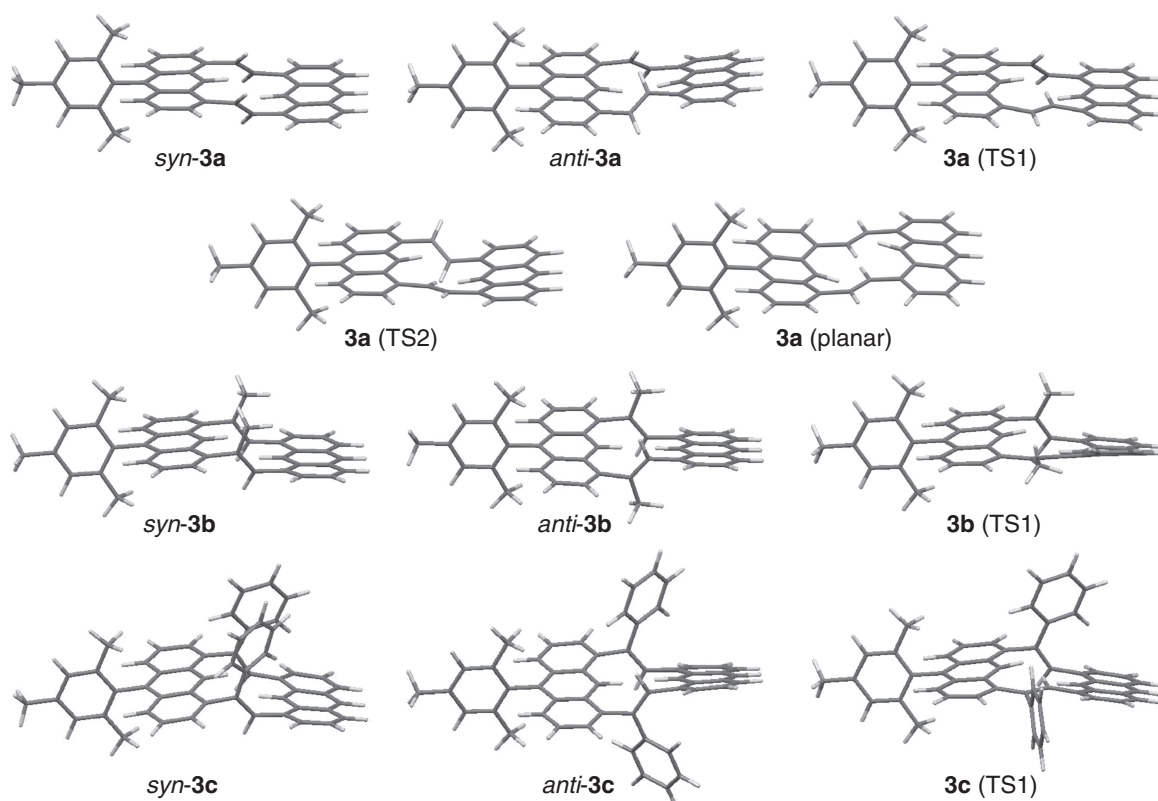


Figure 5. Calculated structures of *syn* and *anti* forms and related structures of **3** optimized at M05/6-31G* level.

Table 2. Relative energies of *syn* and *anti* forms and other related structures of **3** calculated at M05/6-31G* level and observed barriers to dynamic processes

	$E/\text{kJ mol}^{-1}$					Observed barrier / kJ mol^{-1}
	<i>syn</i>	<i>anti</i>	TS1	TS2	planar	
3a	0	9.4	37.6	36.6	61.7	34 (168 K)
3b	0	9.0	72.0	—	—	70 (305 K)
3c	0	11.1	57.1	—	—	55.8 (273 K)

tion spectra of **3** by the TDDFT method. The calculated wavelengths in the p-band region were 447, 397, and 398 nm for **3a**, **3b**, and **3c**, respectively, which were mainly attributed

to the HOMO→LUMO excitation (Supporting Information). The large bathochromic effect of **3a** relative to that of **3b** and **3c** was reasonably reproduced by the theoretical calculation when we compared the peak edge wavelengths in the observed spectra.

Dynamic Behavior. In order to observe the dynamic behavior of macrocyclic compounds **3**, variable temperature (VT) NMR spectra were measured by using the proton signals due to the mesityl group as probe. Because the rotation of the mesityl group relative to the attaching anthracene plane never occurs under ordinary conditions (estimated barrier ca. 200 kJ mol^{-1}),^{9a} the magnetic environment of the two *o*-Me groups is influenced by the conformational preference and the exchange rates (Scheme 2). The two *o*-Me groups are non-

equivalent in the *syn* form of C_s symmetry, whereas they are equivalent in the *anti* form of C_2 symmetry. These signals can be averaged by facile exchange between possible isomers. Although the signals due to *m*-H atoms should exhibit the same behavior, their chemical shift difference was too small to use as an NMR probe.

The VT ^1H NMR spectra were measured in CD_2Cl_2 or toluene- d_8 , depending on the measurable temperature range and the solubility (Figure 7). For **3a**, the *o*-Me groups gave a sharp singlet at room temperature in CD_2Cl_2 , which was unchanged even after lowering the temperature to -83°C . This signal began to broaden at -90°C and decoalesced at -105°C . During the measurements, the other signals showed no significant line shape changes. This observation can be explained by the exchange between the two *syn* forms, which are topomers of each other, via the rotation of the ethylene groups, resulting in the site exchange between Me_A and Me_B , as shown in Scheme 2. Although the exchange was not frozen on the NMR time scale at the lowest attainable temperature, we estimated the barrier to exchange at the coalescence temperature to be $\Delta G^\ddagger_{168} = 34 \text{ kJ mol}^{-1}$.¹⁹

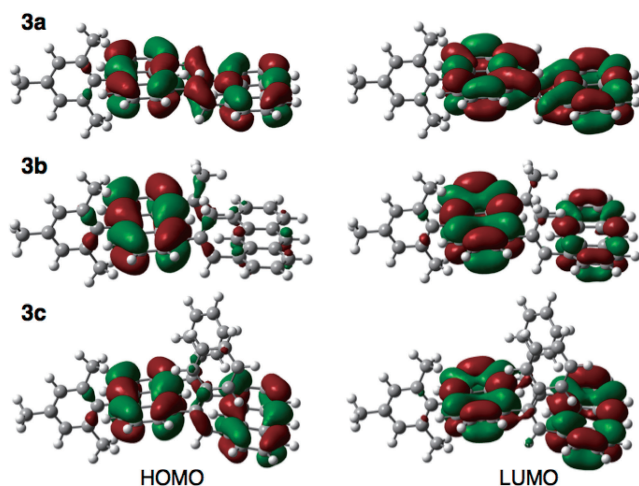
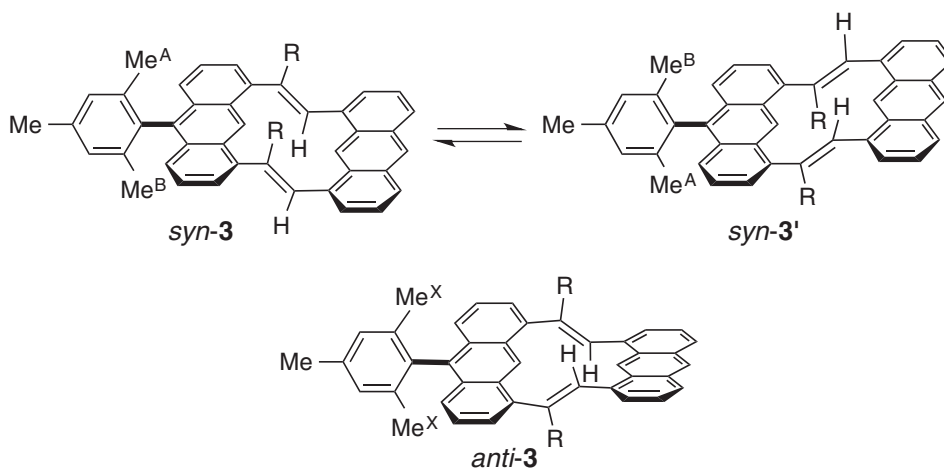


Figure 6. HOMO and LUMO plots of *syn*-**3** calculated at M05/6-31G* level.



Scheme 2. Magnetic equivalence of *o*-Me signals in the mesityl group in *syn*-**3** and *anti*-**3**. Each symbol A, B, or X denotes the *o*-Me groups having the same chemical shift.

The VT ^1H NMR spectra of **3b** and **3c** were measured in toluene- d_8 . For **3c**, the signal due to the *o*-Me group appeared as a broad singlet at room temperature, decoalesced at -2°C , and reshaped into two singlets at -58°C . Total line shape analysis gave the following kinetic parameters: $\Delta H^\ddagger = 53.3 \text{ kJ mol}^{-1}$, $\Delta S^\ddagger = -9.1 \text{ J mol}^{-1} \text{ K}^{-1}$, and $\Delta G^\ddagger_{273} = 55.8 \text{ kJ mol}^{-1}$. For **3b**, the signal was observed as a broad doublet at room temperature, and coalesced at 32°C . Because the chemical shift difference was small (ca. 3 Hz), the barrier to exchange could be approximately determined by the coalescence method, i.e., it was 70 kJ mol^{-1} at 32°C .

The mechanism of the dynamic behavior is discussed on the basis of the above results as well as the additional calculations of transient structures. We propose two discrete mechanisms for the process from the *syn* form to its topomer (Scheme 3). Mechanism A involves the concurrent rotation of the four $\text{C}(\text{arom})\text{-C}(\text{sp}^2)$ bonds through a planar transition state during the topomerization (*syn*-**3** and *syn*-**3'** are topomers of each other). The calculation suggests that the nearly planar structure of **3a** is less stable by ca. 62 kJ mol^{-1} than the global minimum structure (Figure 5 and Table 2). This structure is very unstable because of the steric hindrance between the ethylene and anthracene H atoms in the inner region. As a result, the anthracene moieties suffer from large out-of-plane deformations particularly at the 9-positions. For the substituted derivatives, **3b** and **3c**, the calculations of such structures were impossible because one of the substituents R should be directed into the macrocyclic framework. Therefore, this mechanism is unlikely because the calculated energies are much higher than the observed ones.

Mechanism B proceeds via the stepwise rotation of the two linker moieties, where the rotation of one ethylene moiety in the *syn* form leads to the *anti* form as the intermediate and the following rotation of the other ethylene moiety leads to the *syn* form (Scheme 3). In the transition state, one of the ethylene groups is nearly coplanar with the anthracene planes, where substituent R at the rotating linker is either inside or outside the macrocyclic ring. These two transition state structures, TS1 and TS2, were calculated for each compound (Figure 5). The two structures have comparable energies for **3a**,

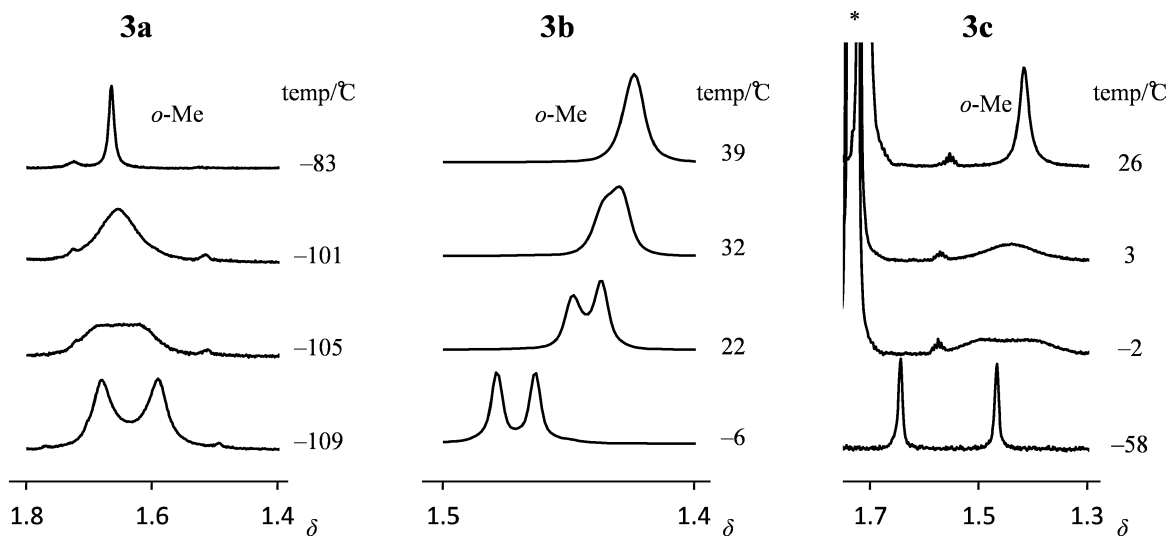
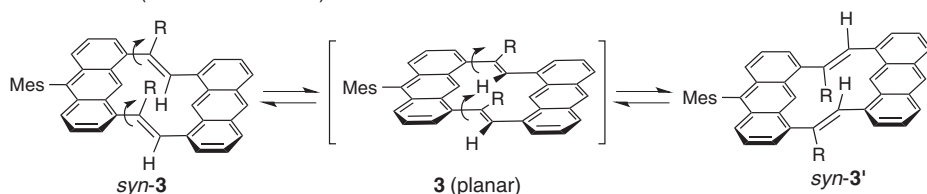
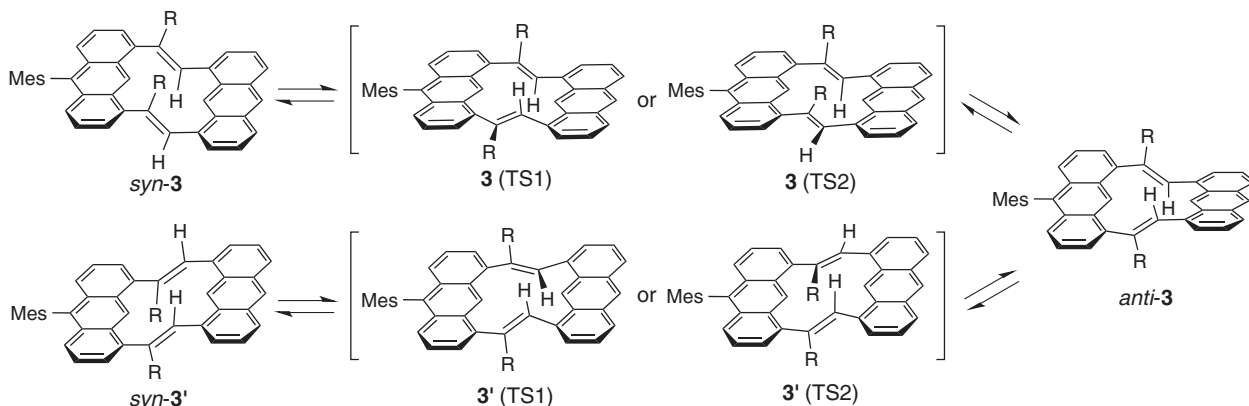


Figure 7. Line shape changes of *o*-Me signals in VT ^1H NMR spectra of **3a** in CD_2Cl_2 and **3b** and **3c** in toluene- d_8 . * Signals due to solvent.

Mechanism A (concurrent rotation)



Mechanism B (stepwise rotation)



Scheme 3. Mechanisms for exchange between two *syn* forms of **3** ($R = \text{H, Me, or Ph}$).

where TS2 is more stable by only 1 kJ mol^{-1} than TS1. Therefore, the rotation can occur via the two transition states. For **3b** and **3c**, the rotation via TS2 is quite unlikely because of the severe steric hindrance of the inside non-hydrogen group R. We were able to obtain only the TS1 structure by optimization as the transition state. Thus calculated barriers, the energy difference between the *syn* form and TS, were 36.6 (**3a**), 72.0 (**3b**), and 57.1 kJ mol^{-1} (**3c**). These values are in good agreement with the experimental barriers determined by VT NMR measurements. These data support mechanism B for the topomerization between the two *syn* forms.

The barrier of **3a** is higher than the barriers to rotation of acyclic *trans*-diarylethenes, for example, *trans*-1,2-diphenyl-

ethene (ca. 16 kJ mol^{-1}).²⁰ In the cyclic system of **3**, the transition state is destabilized by the unavoidable steric interactions in the inner region, which are a kind of transannular interaction. The barriers increase in the order of **3a** ($R = \text{H}$), **3c** (Ph), and **3b** (Me). This tendency can be explained by the steric sizes of H (1.2 \AA), Ph (1.7 \AA), and Me (2.0 \AA), where the van der Waals radii or effective radii are given in parentheses.²¹ The calculated transition state structures suggest that the steric interactions of the outside substituent in the rotating ethylene moiety are important. Figure 8 shows the calculated TS1 structures of **3b** and **3c**. The outside Me or Ph group interacts with aromatic 2-H and 2'-H atoms. The distances between the Me group and the interacting H atoms in **3b**, 2.55 and 2.33 \AA ,

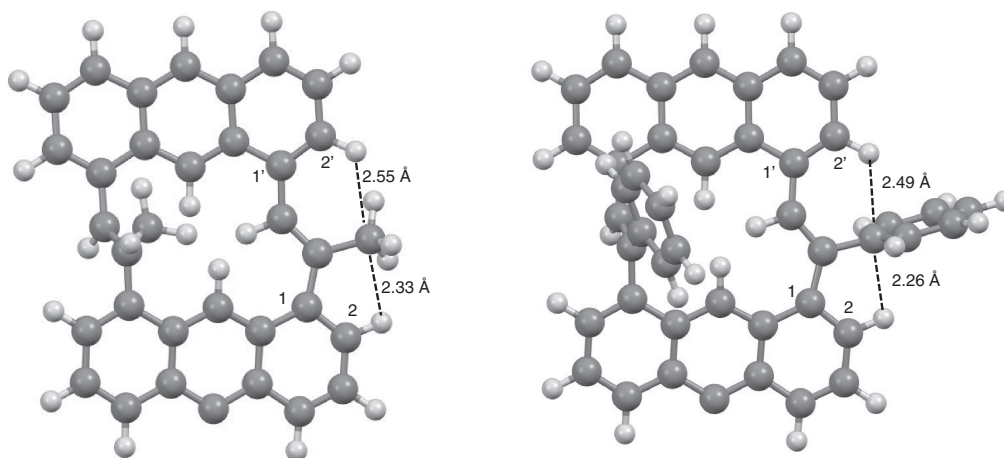


Figure 8. Structures of TS1 of **3b** (left) and **3c** (right). Mesityl groups are omitted for clarity.

are smaller than the sum of radii of the two substituents (3.2 Å). In addition, the anthracene moiety involving C1' and C2' suffers from significant out-of-plane deformation. In TS1 of **3c**, the phenyl group is perpendicular to the linker moiety to minimize the steric hindrance. The distances between the phenyl ipso carbon atom and the interacting H atoms, 2.49 and 2.26 Å, are within the sum of radii (2.9 Å). In this conformation, C–H... π interactions may stabilize the transition state.¹⁷

In summary, macrocyclic compounds consisting of two anthracene units and two ethynylene linkers were synthesized by cross-coupling reactions. The X-ray analysis and DFT calculations revealed that the macrocyclic framework adopted the nonplanar *syn* form. The structures and the electronic properties were influenced by the substituents at the linker moieties, and the Me and Ph substituents decreased the π -conjugation between the anthracene units and the ethynylene linkers due to the large dihedral angles relative to the substituent-free derivative. The dynamic processes between the two *syn* forms were observed from the line shape changes of the *o*-Me signals in the mesityl group in the VT NMR spectra. This topomerization took place by the stepwise rotation of the two ethynylene linkers via the *anti* form as an intermediate, as if the two nonlinear linkers were performing pedaling motion within the cyclic system. The barriers increased in the order of H, Ph, and Me derivatives, corresponding to their steric sizes. These findings indicate that the structures and properties of nonplanar macrocyclic systems can be further modified by introducing substituents at various positions. Further studies of the synthesis of various derivatives involving *cis*-ethynylene linkers or more than two anthracene units are in progress toward creation of novel cyclic systems.

Experimental

General. Melting points are uncorrected. Elemental analyses were performed with a Perkin-Elmer 2400 series analyzer. ¹H and ¹³C NMR spectra were measured on a JEOL JNM-ECS400 spectrometer at 400 and 100 MHz, respectively. Variable temperature ¹H NMR spectra were measured on a JEOL JNM-GSX400 spectrometer at 400 MHz or the JEOL JNM-ECS400 spectrometer. High-resolution mass spectra were measured on a JEOL MStation-700 spectrometer by FAB

method or on a Bruker autoflex speed by MALDI-TOF/TOF method. UV–vis spectra were measured on a Hitachi U-3000 spectrometer with a 10 mm cell. Fluorescence spectra were measured on a JASCO FP-6500 spectrofluorometer with a 10 mm cell with the sample degassed by Ar gas immediately before measurements. Absolute fluorescence quantum yields were recorded on a Hamamatsu photonics C9920-02. Column chromatography was carried out with Merck Silica Gel 60 (70–230 mesh). Boronic acid pinacol esters were purchased from Aldrich.

Compound 6a. 1,8-Diiodoanthracene¹⁰ (**4**, 3.00 g, 6.98 mmol) was dissolved in a mixture of degassed toluene (70 mL) and diisopropylamine (3.92 mL, 27.9 mmol). To the solution were added **5a** (3.58 mL, 20.9 mmol) and [Pd(P^tBu₃)₂] (357 mg, 0.699 mmol). The reaction mixture was heated at 80 °C for 24 h under Ar. After the mixture was filtered through Celite, the filtrate was evaporated. The crude product was purified by chromatography on silica gel with toluene/CH₂Cl₂ 1:1 eluent to give the desired compound as black oil. Yield 2.89 g (86%); ¹H NMR (400 MHz, CDCl₃): δ 1.40 (24H, s), 6.36 (2H, d, J = 18.2 Hz), 7.47 (2H, dd, J = 6.8, 8.0 Hz), 7.75 (2H, d, J = 6.8 Hz), 7.97 (2H, d, J = 8.0 Hz), 8.40 (2H, d, J = 18.2 Hz), 8.44 (1H, s), 9.09 (1H, s); ¹³C NMR (100 MHz, CDCl₃): δ 24.91, 83.35, 118.47, 124.12, 125.26, 127.54, 129.15, 129.53, 131.59, 136.03, 146.65 (one aliphatic signal missing); HRMS (FAB) found: 482.2777 m/z [M]⁺; calcd for C₃₀H₃₆¹¹B₂O₄ m/z 482.2810. The large coupling constant supports *E* stereochemistry for the ethynylene moieties.

1,8-Diiodo-9-mesitylanthracene (8). To a solution of mesitylmagnesium bromide (1 mol L⁻¹ THF solution, 40.4 mL, 40.4 mmol) in THF (100 mL) was added 4,5-diiodo-9-anthrone¹⁰ (3.00 g, 6.73 mmol) under Ar. After the solution was stirred for 24 h at room temperature, the reaction was quenched with NH₄Cl aq (60 mL). The organic layer was separated, and the aqueous layer was extracted with ether (20 mL \times 3). The combined organic layer was dried over MgSO₄ and evaporated. The crude product was purified by chromatography on silica gel with hexane eluent to give the desired compound as a yellow solid. Yield 3.12 g (85%); mp 247–251 °C (dec); ¹H NMR (400 MHz, CDCl₃): δ 1.65 (6H, s), 2.44 (3H, s), 7.05 (2H, dd, J = 6.8, 8.4 Hz), 7.07 (2H, s), 7.48 (2H, d,

$J = 6.8$ Hz), 8.15 (2H, d, $J = 8.4$ Hz), 9.09 (1H, s); ^{13}C NMR (100 MHz, CDCl_3): δ 20.12, 21.38, 100.98, 127.07, 127.16, 128.58, 130.65, 133.24, 133.89, 136.97, 137.51, 137.81, 137.94, 138.13; HRMS (FAB) found: m/z 547.9545 $[\text{M}]^+$; calcd for $\text{C}_{23}\text{H}_{18}\text{I}_2$ m/z 547.9498; Anal found: C, 50.23, H, 3.11%. calcd for $\text{C}_{23}\text{H}_{18}\text{I}_2$: C, 50.39, H, 3.31%.

Cyclic Dimer 3a. To a mixture of degassed toluene (200 mL) and water (20 mL) were added **6a** (10.1 mg, 20.9 μmol , ca. 1.0×10^{-4} mol L $^{-1}$ in toluene), **8** (11.5 mg, 21.0 μmol), Cs_2CO_3 (67.4 mg, 0.21 mmol), and $[\text{Pd}(\text{PPh}_3)_4]$ (2.4 mg, 2.1 μmol). The reaction mixture was heated at 90 °C for 48 h under Ar. After the mixture was filtered through Celite, the organic layer was separated and the aqueous layer was extracted with ether (10 mL \times 3). The combined organic layer was dried over MgSO_4 and evaporated. The crude product was purified by chromatography on silica gel with hexane/ CH_2Cl_2 10:1 eluent to give the desired product (3.6 mg, 33%) as yellow crystals. The yield was 25% when the concentration of **6a** was 1.0×10^{-3} mol L $^{-1}$. Mp 290–301 °C (dec); ^1H NMR (400 MHz, CDCl_3): δ 1.78 (6H, s), 2.48 (3H, s), 7.13 (2H, s), 7.42 (2H, dd, $J = 6.8, 8.8$ Hz), 7.48 (2H, d, $J = 8.8$ Hz), 7.58 (2H, dd, $J = 6.4, 8.4$ Hz), 7.67 (2H, d, $J = 6.8$ Hz), 7.68 (2H, d, $J = 6.4$ Hz), 7.81 (4H, s), 8.04 (2H, d, $J = 8.4$ Hz), 8.56 (1H, s), 10.07 (1H, s), 10.08 (1H, s); ^{13}C NMR (100 MHz, CDCl_3): δ 20.28, 21.42, 121.94, 122.64, 123.91, 125.65, 125.72, 125.75, 127.10, 127.71, 128.47, 130.20, 130.24, 130.34, 132.20, 133.54, 133.76, 136.80, 137.11, 137.23, 137.35, 137.76 (two aromatic signals missing); UV-vis (CHCl_3) λ_{max} (ϵ) 252 (147000), 417 (19000) nm; FL (CHCl_3) λ_{max} 491 nm, λ_{ex} 421 nm, Φ_f 0.71; HRMS (FAB) found: m/z 522.2308 $[\text{M}]^+$; calcd for $\text{C}_{41}\text{H}_{30}$ m/z 522.2348.

Cyclic Dimer 2. This compound was similarly prepared from **6a** (10.1 mg, 20.9 mmol) and **4** (9.1 mg, 21 mmol). The chromatographic purification gave the desired compound as a yellow solid. Yield 2.7 mg (32%); mp 301–310 °C (dec) [ref. >360 °C (dec)]; ^1H NMR (400 MHz, CDCl_3): δ 7.57 (4H, dd, $J = 6.2, 8.0$ Hz), 7.67 (4H, d, $J = 6.2$ Hz), 7.77 (4H, s), 8.03 (4H, d, $J = 8.0$ Hz), 8.55 (2H, s), 10.01 (2H, s); UV-vis (CHCl_3) λ_{max} (ϵ) 250 (133000), 413 (14800) nm; FL (CHCl_3) λ_{max} 484 nm, λ_{ex} 416 nm, Φ_f 0.67; HRMS (MALDI-TOF) found: m/z 404.1565 $[\text{M}]^+$; calcd for $\text{C}_{32}\text{H}_{20}$ 404.1565. The ^{13}C NMR spectrum could not be measured due to the low solubility.

Reaction of 4 and 5b. This coupling reaction was similarly performed by using **4** (100 mg, 0.233 mmol), **5b** (0.131 mL, 0.697 mmol), and $[\text{Pd}(\text{P}^t\text{Bu}_3)_2]$ (11.9 mg, 0.0233 mmol) in toluene (5 mL) and diisopropylamine (0.131 mL, 0.932 mmol) as the synthesis of **3a**. Even though the reaction mixture was heated at 80 °C for 72 h, most of the starting material was recovered. A small amount of the mono-coupling product was obtained: ^1H NMR (400 MHz, CDCl_3): δ 1.40 (12H, s), 1.87 (3H, d, $J = 1.6$ Hz), 7.15 (1H, dd, $J = 7.2, 8.4$ Hz), 7.41 (1H, d, $J = 6.8$ Hz), 7.51 (1H, dd, $J = 7.2, 8.4$ Hz), 7.91 (1H, br), 7.95 (1H, d, $J = 8.4$ Hz), 7.99 (1H, d, $J = 8.0$ Hz), 8.09 (1H, d, $J = 7.6$ Hz), 8.37 (1H, s), 8.77 (1H, s); HRMS (FAB) found: m/z 470.0933 $[\text{M}]^+$; calcd for $\text{C}_{23}\text{H}_{24}^{11}\text{BIO}_2$ m/z 470.0914.

1,8-Bis(1-propynyl)anthracene (7b). To a solution of 1,8-diethynylanthracene²² (1.00 g, 4.42 mmol) in anhydrous THF (100 mL) was slowly added BuLi (1.6 mol L $^{-1}$ hexane solution,

11.1 mL, 17.8 mmol) with a syringe at -78 °C under Ar. After this solution was stirred at that temperature for 1 h, MeI (2.75 mL, 44.2 mmol) was added. The solution was stirred at that temperature for 1 h, and then at room temperature for 1 h. The reaction mixture was treated with aq. NH_4Cl (20 mL), and the organic solvents were evaporated. The organic materials were extracted with CH_2Cl_2 (20 mL \times 3). The combined organic layer was dried over MgSO_4 and evaporated. The crude product was purified by chromatography on silica gel with hexane/ CH_2Cl_2 3:1 eluent to give the desired compound as a yellow solid. Yield 1.04 g (93%); mp 200–203 °C; ^1H NMR (400 MHz, CDCl_3): δ 2.30 (6H, s), 7.40 (2H, dd, $J = 6.8, 8.8$ Hz), 7.63 (2H, d, $J = 6.8$ Hz), 7.95 (2H, d, $J = 8.8$ Hz), 8.40 (1H, s), 9.40 (1H, s); ^{13}C NMR (100 MHz, CDCl_3): δ 4.81, 78.17, 91.50, 122.37, 124.37, 125.21, 127.20, 128.24, 129.69, 131.60, 131.93; HRMS (FAB) found 254.1081 m/z $[\text{M}]^+$; calcd for $\text{C}_{20}\text{H}_{14}$ m/z 254.1096; Anal found: C, 94.05, H, 5.73%. calcd for $\text{C}_{20}\text{H}_{10}$: C, 94.45, H, 5.55%.

Compound 6b. A mixture of CuCl (19.5 mg, 0.197 mmol), NaO t Bu (75.7 mg, 0.788 mmol), and PPh $_3$ (103 mg, 0.393 mmol) was suspended in THF (25 mL) under Ar. After this mixture was stirred for 30 min, bis(pinacolato)diboron (1.50 g, 5.91 mmol) was added. After this mixture was further stirred for 10 min, **7** (500 mg, 1.97 mmol) and MeOH (0.64 mL, 16 mmol) were added. The reaction mixture was heated at 50 °C for 1 h, and then filtered through Celite. The filtrate was evaporated, and the residue was dissolved in CHCl_3 (20 mL). This organic layer was washed with 1 mol L $^{-1}$ aq. HCl (10 mL \times 3) and aq. NaCl (10 mL), dried over MgSO_4 , and evaporated. The crude product was purified by chromatography on silica gel with hexane/ethyl acetate 40:1 eluent to give the desired product as brown oil. Yield 932 mg (93%); ^1H NMR (400 MHz, CDCl_3): δ 1.37 (24H, s), 1.87 (6H, s), 7.34 (2H, d, $J = 6.8$ Hz), 7.44 (2H, dd, $J = 6.8, 8.4$ Hz), 7.82 (2H, s), 7.93 (2H, d, $J = 8.4$ Hz), 8.44 (1H, s), 8.54 (1H, s); ^{13}C NMR (100 MHz, CDCl_3): δ 16.74, 25.09, 83.57, 121.45, 124.83, 126.65, 127.46, 127.87, 130.16, 131.77, 135.76, 141.33 (one aliphatic signal missing); HRMS (FAB) found 510.3113 m/z $[\text{M}]^+$; calcd for $\text{C}_{32}\text{H}_{40}^{11}\text{B}_2\text{O}_4$ m/z 510.3113.

Cyclic Dimer 3b. This compound was similarly synthesized from **6b** (10.0 mg, 19.6 μmol), **8** (10.7 mg, 19.5 μmol), Cs_2CO_3 (63.6 mg, 0.195 mmol), and $[\text{Pd}(\text{PPh}_3)_4]$ (2.25 mg, 1.95 μmol) as the synthesis of **3a**. The crude product was purified by chromatography on silica gel with hexane/ CH_2Cl_2 10:1 eluent to give the desired product as yellow solid. The yield was 5.5 mg (51%) at ca. 1.0×10^{-4} mol L $^{-1}$ and 4.3 mg (40%) at ca. 1.0×10^{-3} mol L $^{-1}$. Mp 167–169 °C; ^1H NMR (400 MHz, CDCl_3): δ 1.81 (6H, s), 2.10 (6H, s), 2.49 (3H, s), 7.31 (2H, s), 7.15 (2H, s), 7.40 (2H, dd, $J = 6.4, 8.8$ Hz), 7.48 (2H, d, $J = 8.8$ Hz), 7.51–7.53 (4H, m), 7.58 (2H, dd, $J = 6.8, 8.8$ Hz), 8.05 (2H, d, $J = 8.0$ Hz), 8.57 (1H, s), 9.62 (2H, s); ^{13}C NMR (100 MHz, CDCl_3): δ 20.38, 21.02, 21.43, 122.94, 123.66, 123.82, 125.25, 125.33, 125.51, 126.97, 127.29, 128.43, 129.23, 130.14, 130.18, 130.76, 132.03, 135.17, 136.56, 136.76, 137.26, 137.84, 141.47, 143.89 (one aromatic signal missing); UV-vis (CHCl_3) λ_{max} (ϵ) 254 (141000), 359 (9240), 378 (15500), 398 (16500) nm; FL (CHCl_3) λ_{max} 438 nm, λ_{ex} 398 nm, Φ_f 0.82; HRMS (FAB) found 550.2659 m/z $[\text{M}]^+$; calcd for $\text{C}_{43}\text{H}_{34}$ m/z 550.2661.

Reaction of 4 and 5c. This reaction was similarly performed with **4** (300 mg, 0.698 mmol), **5c** (483 mg, 2.10 mmol), and [Pd(P^tBu₃)₂] (35.7 mg, 0.0699 mmol) in toluene (15 mL) and diisopropylamine (0.39 mL, 2.77 mmol) as the synthesis of **6a**. The crude product was purified by chromatography on silica gel with hexane/ethyl acetate 5:1 to give compound **6c'** (*E/E* product) as a brown solid. The stereochemistry was confirmed by X-ray analysis (Figure S3). Yield 342 mg (77%); mp 172–174 °C; ¹H NMR (400 MHz, CDCl₃): δ 1.11 (24H, s), 7.28–7.33 (6H, m), 7.42 (2H, dd, *J* = 6.8, 8.8 Hz), 7.58–7.60 (6H, m), 7.95 (2H, d, *J* = 8.8 Hz), 8.03 (2H, s), 8.43 (1H, s), 8.96 (1H, s); ¹³C NMR (100 MHz, CDCl₃): δ 24.80, 83.93, 121.88, 125.04, 125.31, 127.01, 127.07, 127.25, 128.20, 128.62, 130.50, 131.76, 137.26, 138.64, 142.40 (one aliphatic signal missing); HRMS (FAB) found 634.3436 *m/z* [M]⁺; calcd for C₄₂H₄₄¹¹B₂O₄ *m/z* 634.3426.

Compound 6c. This compound was similarly prepared from **7c**¹⁰ (900 mg, 2.38 mmol), bis(pinacolato)diboron (1.81 g, 7.13 mmol), CuCl (23.6 mg, 0.238 mmol), NaO^tBu (91.5 mg, 0.952 mmol), PPh₃ (125 mg, 0.477 mmol), and MeOH (769 μL, 19.0 mmol) in THF (45 mL) as the synthesis of **6b**. The crude product was purified by chromatography on silica gel with CHCl₃ eluent to give the desired product as a yellow solid. Yield 421 mg (28%); Mp 208–211 °C; ¹H NMR (400 MHz, CDCl₃): δ 1.42 (24H, s), 7.00–7.11 (12H, m), 7.18 (2H, dd, *J* = 7.2, 8.4 Hz), 7.79 (2H, d, *J* = 8.4 Hz), 7.97 (2H, s), 8.33 (1H, s), 8.55 (1H, s); ¹³C NMR (100 MHz, CDCl₃): δ 25.13, 83.98, 121.39, 124.85, 126.23, 127.54, 127.89, 127.94, 127.99, 129.68, 131.61, 135.85, 140.30, 142.68 (one aliphatic signal and one aromatic signal missing); HRMS (FAB) found 634.3464 *m/z* [M]⁺; calcd for C₄₂H₄₄B₂O₄ *m/z* 634.3426. This reaction also gave several other isomers, which were not separable by conventional chromatography.

Cyclic Dimer 3c. This compound was similarly synthesized from **6c** (10.0 mg, 15.8 μmol), **8** (8.68 mg, 15.8 μmol), Cs₂CO₃ (51.3 mg, 0.157 mmol), and [Pd(PPh₃)₄] (1.83 mg, 1.58 μmol) as the synthesis of **3a**. The crude product was purified by chromatography on silica gel with hexane/CH₂Cl₂ 10:1 eluent to give the desired product as yellow solid. The yield was 6.7 mg (63%) at ca. 1.0 × 10⁻⁴ mol L⁻¹ and 5.7 mg (54%) at ca. 1.0 × 10⁻³ mol L⁻¹. Mp 300–310 °C (dec); ¹H NMR (400 MHz, CDCl₃): δ 1.81 (6H, s), 2.48 (3H, s), 6.76 (4H, t, *J* = 8.0 Hz), 6.89 (2H, t, *J* = 7.2 Hz), 7.02 (4H, d, *J* = 8.0 Hz), 7.13 (2H, s), 7.37 (2H, s), 7.42–7.50 (8H, m), 7.66 (2H, d, *J* = 6.4 Hz), 7.99 (2H, d, *J* = 8.4 Hz), 8.51 (1H, s), 9.77 (1H, s), 9.86 (1H, s); ¹³C NMR (100 MHz, CDCl₃): δ 20.52, 21.44, 123.92, 124.47, 124.99, 125.40, 125.45, 125.58, 125.72, 126.98, 127.29, 127.82, 128.45, 130.17, 131.02, 131.19, 131.38, 131.90, 135.07, 136.49, 136.75, 137.29, 137.90, 138.74, 142.33, 143.72 (two aromatic signals missing); UV-vis (CHCl₃) λ_{max} (ε) 255 (123000), 360 (10400), 379 (17000), 400 (17000) nm; FL (CHCl₃) λ_{max} 478 nm, λ_{ex} 377 nm, Φ_F 0.39; HRMS (FAB) found 674.2988 *m/z* [M]⁺; calcd for C₅₃H₃₈ *m/z* 674.2974.

VT NMR Measurements. ¹H NMR spectra were measured at variable temperatures in toluene-*d*₈ (**3b** and **3c**) or in CD₂Cl₂ (**3a**) on a JEOL JNM-ECS400 spectrometer at 400 MHz (Figure S1). The sample temperature was monitored by a thermocouple after calibration with the ¹H NMR chemical

shifts of a methanol sample or a 1,2-ethanediol sample. For **3a**, the signal due to the *o*-Me groups decoalesced at –105 °C (168 K). The chemical shift difference (Δ*ν*/Hz) was estimated to be 42 Hz, even though the signals were still broad at –109 °C, the lowest attainable temperature. The rate constant at the coalescence temperature (*T*_c) was calculated by the empirical equation for the coalescence method, *k* = (π/√2) · Δ*ν*, to be *k* = 152 s⁻¹.¹⁹ This value corresponded to the free energy of activation Δ*G*[‡] at *T*_c to be 34 kJ mol⁻¹. For **3b**, the *o*-Me signals coalesced at 32 °C (305 K) and the Δ*ν* was approximately 3 Hz. These values afforded *k* = 6.7 s⁻¹ and Δ*G*[‡] = 70 kJ mol⁻¹ at *T*_c in a similar manner. The total line shape analyses of the *o*-Me signals of **3c** were performed by the DNMR3K program (Figure S2).²³ The line shape changes were analyzed as 2-site mutual exchanges (A ⇌ X). The chemical shift difference (Δ*ν*) was assumed to be a linear function of the temperature (*t*/°C) as Δ*ν* = –0.247 *t* + 56.9 (Hz), and the spin-spin relaxation time (*T*₂/s) was fixed at 0.06. Rate constants are as follows: *k*/s⁻¹ (*t*/°C) = 15 (–21.7), 25 (–16.5), 40 (–11.4), 65 (–6.5), 100 (–1.5), 170 (3.3), 250 (8.1), 350 (12.7). The Eyring plot of these data afforded the following kinetic parameters: Δ*H*[‡] = (53.3 ± 1.8) kJ mol⁻¹, Δ*S*[‡] = (–9.1 ± 6.7) J mol⁻¹ K⁻¹, Δ*G*[‡]₂₇₃ = (55.8 ± 3.8) kJ mol⁻¹.

DFT Calculations. Calculations were carried out with Gaussian 09²⁴ program on a Windows computer. The structures were optimized by the hybrid DFT method at the M05/6-31G* level. The frequency analysis gave no imaginary frequency for each energy minimum structure, one imaginary frequency for transition state structure, and two imaginary frequencies for nearly planar structure. The calculations of excited states were carried out by the TDDFT method at the same level.

X-ray Analysis. Single crystals of **3** and **2** were obtained by crystallization from suitable solvents. Diffraction data were collected on a Rigaku Varimax imaging plate diffractometer with Mo Kα radiation (λ = 0.71075 Å) to a maximum 2θ value of 55.0° at –150 °C. The structure was solved by the direct method (SHELXS97)²⁵ and refined by the full-matrix least squares method (SHELXL97).²⁶ Non-hydrogen atoms were refined anisotropically. Hydrogen atoms were included in fixed positions. Copies of the data can be obtained free of charge via <http://www.ccdc.cam.ac.uk/conts/retrieving.html> (or from the Cambridge Crystallographic Data Centre, 12, Union Road, Cambridge, CB2 1EZ, UK; Fax: +44 1223 762911; e-mail: deposit@ccdc.cam.ac.uk). **3a** (CCDC 953893): Recrystallized from benzene/ethanol. Formula (C₄₁H₃₀)·0.25(C₆H₆), *M* = 1084.35, triclinic, *P* $\bar{1}$, *a* = 11.130(2), *b* = 15.080(3), *c* = 18.842(4) Å, α = 100.300(12), β = 92.311(17), γ = 110.700(9)°, *V* = 2892.3(11) Å³, *Z* = 4, *D*_c = 1.245 g cm⁻³, μ(Mo Kα) = 0.070 mm⁻¹. Number of data 24518, number of data used 12959 [*I* > 2.0σ(*I*)], *R*1 = 0.0890, *wR*2 = 0.1801, GOF = 1.075. CCDC 953893. **3b** (CCDC 1407436): Recrystallized from benzene/ethanol. Formula C₄₃H₃₄ 1.5(C₆H₆), *M* = 667.86, triclinic, *P* $\bar{1}$, *a* = 10.318(3), *b* = 12.288(3), *c* = 15.711(4) Å, α = 102.516(3), β = 90.952(3), γ = 109.733(3)°, *V* = 1821.7(8) Å³, *Z* = 2, *D*_c = 1.218 g cm⁻³, μ(Mo Kα) = 0.069 mm⁻¹. Number of data 16025, number of data used 8187 [*I* > 2.0σ(*I*)], *R*1 = 0.0528, *wR*2 = 0.1268, GOF = 1.055. **3c** (CCDC 1407435): Recrystallized from benzene/ethanol. Formula (C₅₃H₃₈)·1.5(C₆H₆), *M* = 792.00, triclinic,

$P\bar{1}$, $a = 10.0012(13)$, $b = 14.897(2)$, $c = 29.721(4)$ Å, $\alpha = 80.707(4)$, $\beta = 84.409(5)$, $\gamma = 83.905(5)^\circ$, $V = 4330.5(10)$ Å³, $Z = 4$, $D_c = 1.215$ g cm⁻³, $\mu(\text{Mo K}\alpha) = 0.069$ mm⁻¹. Number of data 38314, number of data used 19509 [$I > 2.0\sigma(I)$], $R1 = 0.0756$, $wR2 = 0.1512$, $\text{GOF} = 1.071$. **2** (CCDC 1407434): Recrystallized from chlorobenzene. Formula C₃₂H₂₀, $M = 404.48$, triclinic, $P\bar{1}$, $a = 7.294(2)$, $b = 10.142(3)$, $c = 13.847(4)$ Å, $\alpha = 95.757(5)$, $\beta = 92.502(5)$, $\gamma = 101.972(5)^\circ$, $V = 994.9(5)$ Å³, $Z = 2$, $D_c = 1.350$ g cm⁻³, $\mu(\text{Mo K}\alpha) = 0.076$ mm⁻¹. Number of data 8798, number of data used 4497 [$I > 2.0\sigma(I)$], $R1 = 0.0514$, $wR2 = 0.1188$, $\text{GOF} = 1.017$.

This work was partly supported by MEXT KAKENHI for Scientific Research on Innovative Areas (Integrated Organic Synthesis) Grant Number 24106743, JSPS KAKENHI for Scientific Research (C) Grant Number 26410060, and by a MEXT-Supported Program for the Strategic Research Foundation at Private Universities, 2009–2013.

Supporting Information

¹H (VT) and ¹³C NMR of **3**, X-ray structure of **6c'**, and DFT calculation data of **3**. This material is available electronically on J-STAGE.

References and Notes

- 1 A part of this work was preliminarily reported as a communication: M. Inoue, T. Iwanaga, S. Toyota, *Chem. Lett.* **2013**, *42*, 1499.
- 2 a) S. Toyota, *Pure Appl. Chem.* **2012**, *84*, 917. b) S. Toyota, *Chem. Lett.* **2011**, *40*, 12. c) S. Toyota, M. Goichi, M. Kotani, *Angew. Chem., Int. Ed.* **2004**, *43*, 2248.
- 3 a) S. Toyota, M. Kurokawa, M. Araki, K. Nakamura, T. Iwanaga, *Org. Lett.* **2007**, *9*, 3655. b) T. Iwanaga, K. Miyamoto, K. Tahara, K. Inukai, S. Okuhata, Y. Tobe, S. Toyota, *Chem.—Asian J.* **2012**, *7*, 935.
- 4 Examples of other dimers involving diacetylene linkers. a) W. Zhao, Q. Tang, H. S. Chan, J. Xu, K. Y. Lo, Q. Miao, *Chem. Commun.* **2008**, 4324. b) S. Toyota, H. Onishi, Y. Kawai, T. Morimoto, H. Miyahara, T. Iwanaga, K. Wakamatsu, *Org. Lett.* **2009**, *11*, 321. c) S. Toyota, H. Onishi, K. Wakamatsu, T. Iwanaga, *Chem. Lett.* **2009**, *38*, 350. d) T. Tsuya, K. Iritani, K. Tahara, Y. Tobe, T. Iwanaga, S. Toyota, *Chem.—Eur. J.* **2015**, *21*, 5520.
- 5 a) W. B. Davis, W. A. Svec, M. A. Ratner, M. R. Wasielewski, *Nature* **1998**, *396*, 60. b) R. Schenk, H. Gregorius, K. Meerholz, J. Heinze, K. Müllen, *J. Am. Chem. Soc.* **1991**, *113*, 2634. c) R. Schenk, H. Gregorius, K. Müllen, *Adv. Mater.* **1991**, *3*, 492. d) M. Rumi, J. E. Ehrlich, A. A. Heikal, J. W. Perry, S. Barlow, Z. Hu, D. McCord-Maughon, T. C. Parker, H. Röckel, S. Thayumanavan, S. R. Marder, D. Beljonne, J.-L. Brédas, *J. Am. Chem. Soc.* **2000**, *122*, 9500. e) Z. Zhu, T. M. Swager, *J. Am. Chem. Soc.* **2002**, *124*, 9670. f) H. Meier, J. Gerold, H. Kolshorn, W. Baumann, M. Bletz, *Angew. Chem., Int. Ed.* **2002**, *41*, 292. g) A. Gesquière, P. Jonkheijm, F. J. M. Hoeben, A. P. H. J. Schenning, S. De Feyter, F. C. De Schryver, E. W. Meijer, *Nano Lett.* **2004**, *4*, 1175. h) H. Wang, H. H. Wang, V. S. Urban, K. C. Littrell, P. Thiyagarajan, L. Yu, *J. Am. Chem. Soc.* **2000**, *122*, 6855.
- 6 a) M. Yoshizawa, J. K. Klosterman, *Chem. Soc. Rev.* **2014**, *43*, 1885. b) A. R. Mohebbi, E.-K. Mucke, G. R. Schaller, F.

Köhler, F. D. Sönnichsen, L. Ernst, C. Näther, R. Herges, *Chem.—Eur. J.* **2010**, *16*, 7767. c) S. Heun, H. Bässler, U. Müller, K. Müllen, *J. Phys. Chem.* **1994**, *98*, 7355. d) A. Bohnen, H. J. Räder, K. Müllen, *Synth. Met.* **1992**, *47*, 37. e) H.-P. Weitzel, A. Bohnen, K. Müllen, *Makromol. Chem.* **1990**, *191*, 2815. f) S. Nakatsuji, K. Matsuda, Y. Uesugi, K. Nakashima, S. Akiyama, G. Katzer, W. Fabian, *J. Chem. Soc., Perkin Trans. 2* **1991**, 861.

7 S. Akiyama, M. Nakagawa, *Bull. Chem. Soc. Jpn.* **1971**, *44*, 3158.

8 a) M. Yoshikawa, S. Imigi, K. Wakamatsu, T. Iwanaga, S. Toyota, *Chem. Lett.* **2013**, *42*, 559. b) A. Konishi, Y. Hirao, K. Matsumoto, H. Kurata, R. Kishi, Y. Shigeta, M. Nakano, K. Tokunaga, K. Kamada, T. Kubo, *J. Am. Chem. Soc.* **2013**, *135*, 1430. c) Y. Fujiwara, R. Ozawa, D. Onuma, K. Suzuki, K. Yoza, K. Kobayashi, *J. Org. Chem.* **2013**, *78*, 2206.

9 a) S. Toyota, T. Oki, M. Inoue, K. Wakamatsu, T. Iwanaga, *Chem. Lett.* **2015**, *44*, 978. b) K. Nikitin, H. Müller-Bunz, Y. Ortin, J. Muldoon, M. J. McGlinchey, *Org. Lett.* **2011**, *13*, 256. c) D. Nori-shargh, S. Asadzadeh, F.-R. Ghanizadeh, F. Deyhimi, M. M. Amini, S. Jameh-Bozorgi, *THEOCHEM* **2005**, *717*, 41.

10 M. Goichi, K. Segawa, S. Suzuki, S. Toyota, *Synthesis* **2005**, 2116.

11 a) K. Itami, K. Tonogaki, T. Nokami, Y. Ohashi, J. Yoshida, *Angew. Chem., Int. Ed.* **2006**, *45*, 2404. b) K. Itami, K. Tonogaki, Y. Ohashi, J. Yoshida, *Org. Lett.* **2004**, *6*, 4093.

12 The stereochemistry of **6c'** was confirmed by the X-ray analysis. The observed structure is given in Supporting Information.

13 a) C. E. Tucker, J. Davidson, P. Knochel, *J. Org. Chem.* **1992**, *57*, 3482. b) M. Haberberger, S. Enthaler, *Chem.—Asian J.* **2013**, *8*, 50.

14 H. R. Kim, J. Yun, *Chem. Commun.* **2011**, *47*, 2943.

15 In a derivative of **3a** (Ph instead of Mes), the coupling constant between the ethylene protons ($J = 16.8$ Hz) was observable in the ¹H NMR spectrum, being typical for the *trans* relationship. See ref. 1.

16 a) B. Valeur, M. N. Berberan-Santos, *Molecular Fluorescence: Principles and Applications*, 2nd ed., Wiley-VCH, Weinheim, **2012**, Chap. 9.5. b) M. Levitus, M. A. Garcia-Garibay, *J. Phys. Chem. A* **2000**, *104*, 8632.

17 M. Nishio, M. Hirota, Y. Umezawa, *The CH/π Interaction: Evidence, Nature, and Consequences*, Wiley-VCH, New York, **1998**.

18 a) Y. Zhao, D. G. Truhlar, *Acc. Chem. Res.* **2008**, *41*, 157. b) S. Toyota, K. Wakamatsu, T. Kawakami, T. Iwanaga, *Bull. Chem. Soc. Jpn.* **2015**, *88*, 283.

19 M. Ōki, *Applications of Dynamic NMR Spectroscopy to Organic Chemistry*, VCH, Deerfield Beach, **1985**.

20 S. P. Kwasniewski, L. Claes, J.-P. François, M. S. Deleuze, *J. Chem. Phys.* **2003**, *118*, 7823.

21 a) G. Bott, L. D. Field, S. Sternhell, *J. Am. Chem. Soc.* **1980**, *102*, 5618. b) A. Bondi, *J. Phys. Chem.* **1964**, *68*, 441. c) A. Bondi, *J. Phys. Chem.* **1966**, *70*, 3006.

22 H. E. Katz, *J. Org. Chem.* **1989**, *54*, 2179.

23 DNMR3K program. G. Binsch, *Top. Stereochem.* **1968**, *3*, 97; D. Kleier, G. Binsch, *QCPE #165*, Indiana University, Bloomington, IN, USA.

24 M. J. Frisch, G. W. Trucks, H. B. Schlegel, G. E. Scuseria, M. A. Robb, J. R. Cheeseman, G. Scalmani, V. Barone, B. Mennucci, G. A. Petersson, H. Nakatsuji, M. Caricato, X. Li, H. P. Hratchian, A. F. Izmaylov, J. Bloino, G. Zheng, J. L. Sonnenberg, M. Hada, M. Ehara, K. Toyota, R. Fukuda, J. Hasegawa, M. Ishida,

- T. Nakajima, Y. Honda, O. Kitao, H. Nakai, T. Vreven, J. A. Montgomery, Jr., J. E. Peralta, F. Ogliaro, M. Bearpark, J. J. Heyd, E. Brothers, K. N. Kudin, V. N. Staroverov, R. Kobayashi, J. Normand, K. Raghavachari, A. Rendell, J. C. Burant, S. S. Iyengar, J. Tomasi, M. Cossi, N. Rega, J. M. Millam, M. Klene, J. E. Knox, J. B. Cross, V. Bakken, C. Adamo, J. Jaramillo, R. Gomperts, R. E. Stratmann, O. Yazyev, A. J. Austin, R. Cammi, C. Pomelli, J. W. Ochterski, R. L. Martin, K. Morokuma, V. G. Zakrzewski, G. A. Voth, P. Salvador, J. J. Dannenberg, S. Dapprich, A. D. Daniels, Ö. Farkas, J. B. Foresman, J. V. Ortiz, J. Cioslowski, D. J. Fox, *Gaussian 09 (Revision C.01)*, Gaussian, Inc., Wallingford CT, **2009**.
- 25 G. M. Sheldrick, SHELXS-97, *Program for the Solution of Crystal Structures*, University of Göttingen, Germany, **1997**.
- 26 G. M. Sheldrick, SHELXL-97, *Program for the Refinement of Crystal Structures*, University of Göttingen, Germany, **1997**.